

Exclusive and semiexclusive production of $\mu^+\mu^-$ pairs with Δ isobars and other resonances in the final state and the size of absorption effects

Piotr Lebiedowicz^{1,*} and Antoni Szczurek^{+1,‡}

¹*Institute of Nuclear Physics Polish Academy of Sciences,
ul. Radzikowskiego 152, PL-31-342 Kraków, Poland*

Abstract

We include $pp \rightarrow p\Delta^+\mu^+\mu^-$ and $pp \rightarrow \Delta^+\Delta^+\mu^+\mu^-$ processes in addition to the standard $pp \rightarrow pp\mu^+\mu^-$ process both in equivalent-photon approximation (EPA) and in exact $2 \rightarrow 4$ calculations. For comparison we calculate also the continuum proton dissociation in a recently developed k_t -factorization approach to $\gamma\gamma$ -involved processes with parametrizations of F_2 structure function known from the literature. The calculated cross section including all the processes is considerably larger than the one measured recently by the ATLAS collaboration. We calculate absorption effects for $pp \rightarrow pp\mu^+\mu^-$ process in the momentum space. The final cross section with absorption effects is by 10% larger than the one measured by the ATLAS collaboration which is difficult to explain. Several differential distributions with the ATLAS experimental cuts are presented. It is shown that the processes with electromagnetic $p \rightarrow \Delta(1232)$ and $p \rightarrow N(1440)$ transitions, that have similar characteristics as the $pp \rightarrow pp\mu^+\mu^-$ process, increase the cross section for $\mu^+\mu^-$ production and thus can affect its theoretical interpretation when the leading baryons are not detected as is the case for the CMS and ATLAS measurements. The mechanism of dissociation into hadronic continuum is not under full control as the corresponding absorption effects are not fully understood. We present first predictions for future ATLAS experiment with the ALFA sub-detectors and discuss observables relevant for this measurement.

⁺ Also at *Faculty of Mathematics and Natural Sciences, University of Rzeszów, ul. Pigonia 1, PL-35-310 Rzeszów, Poland.*

*Electronic address: Piotr.Lebiedowicz@ifj.edu.pl

‡Electronic address: Antoni.Szczurek@ifj.edu.pl

I. INTRODUCTION

Recently the ATLAS collaboration measured production of muon pairs with the requirement of rapidity gap and small transverse momentum of the dimuon system at proton-proton collision energy $\sqrt{s} = 13$ TeV [1]. A similar study was done previously at $\sqrt{s} = 7$ TeV [2–4]. There have been also efforts to install and use forward proton detectors, see e.g. [5]. In order to ensure the exclusivity of dimuon measurement [1] the measurement was performed for a dimuon invariant mass of $12 \text{ GeV} < M_{\mu^+\mu^-} < 70 \text{ GeV}$ with different $p_{t,\mu}$ conditions and the muon pair was required to have a transverse momentum $p_{t,\mu^+\mu^-} < 1.5 \text{ GeV}$. It is believed that such requirements cause that the cross section is dominated by the $pp \rightarrow pp\mu^+\mu^-$ fully exclusive contribution.

The common approach to calculate cross sections for photon induced processes is the equivalent-photon approximation (EPA). The ATLAS collaboration observed significantly lower cross section than that predicted by the EPA approach [1]. The effect could be caused by absorption effects which destroy rapidity gaps. The absorption effects can be calculated in the momentum space (see e.g. [6–8]) or in the impact parameter space (see e.g. [9]). Only very few differential distributions can be obtained in the EPA approach. In the impact parameter space approach the situation is similar [9]. However, experimental cuts on (pseudo)rapidities and transverse momenta of muons selected only some kinematical configurations, so the use of the phase space averaged value of the gap survival factor may be not justified. Moreover, the effect of absorption strongly depends on kinematics of outgoing protons [7, 10]. Therefore in the following we perform precise calculation of the exclusive $2 \rightarrow 4$ process (8-fold phase space integration) as is routinely done for instance for the $pp \rightarrow pp\pi^+\pi^-$ reaction [11–13], for the $pp \rightarrow ppK^+K^-$ reaction [14, 15] or for the $pp \rightarrow ppp\bar{p}$ reaction [16].

The exclusive $pp \rightarrow pp\mu^+\mu^-$ process competes with the two-photon interactions involving single- and double-proton dissociation contributions. The ATLAS experiment imposes a rather loose cut on $p_{t,\mu^+\mu^-} < 1.5 \text{ GeV}$ [1]. To which extend such a loose cut allows participation of other mechanisms such a single or double proton resonance production? The inclusion of Δ isobar seems potentially the most important. The electromagnetic production of one Δ resonances on either leg or simultaneous excitation of two Δ resonances on both legs was never discussed quantitatively in the context of semiexclusive production of dilepton pairs. EPA fluxes of photons associated with Δ production were presented in [17]. They were used only in [18] for the $pp \rightarrow p\Delta J/\psi$ process. Semiexclusive processes with the Δ excitations for the J/ψ production were estimated also in [19].

During the last years several authors have discussed the backgrounds for the process $pp \rightarrow pp(\gamma\gamma \rightarrow \mu^+\mu^-)$. In particular, the contribution of the semielastic and inelastic $\mu^+\mu^-$ production, where one or both protons dissociate, have been analyzed in [20–23]. The proton-dissociative processes have significantly different kinematic distributions compared to the elastic (purely exclusive) process, which allows in principle for a separation of the different production mechanisms.

In the present paper we wish to consider the $pp \rightarrow p\Delta\mu^+\mu^-$ and $pp \rightarrow \Delta\Delta\mu^+\mu^-$ processes both in EPA and in exact $2 \rightarrow 4$ calculation in addition to the standard $pp \rightarrow pp\mu^+\mu^-$ process. For reference we shall include also production of Roper resonance ($N(1440)$) for which some knowledge is available from the studies with the CLAS detector at the Thomas Jefferson National Accelerator Facility (JLab) [24, 25]. In the fol-

lowing we wish to discuss absorption effects for the $2 \rightarrow 4$ processes considered. We wish to estimate also the role of electromagnetically induced proton-dissociative processes ($pp \rightarrow pX\mu^+\mu^-$ and $pp \rightarrow XY\mu^+\mu^-$) calculated in a recently developed k_t -factorization approach using the phenomenological parametrizations of the deep-inelastic structure functions from the literature.

II. THEORETICAL APPROACH

In Fig. 1 we show “Born level” diagrams of processes considered in the present analysis for central exclusive $\mu^+\mu^-$ production in proton-proton collisions:

$$p + p \rightarrow p + \mu^+ + \mu^- + p, \quad (2.1)$$

$$p + p \rightarrow p + \mu^+ + \mu^- + \Delta^+, \quad (2.2)$$

$$p + p \rightarrow \Delta^+ + \mu^+ + \mu^- + p, \quad (2.3)$$

$$p + p \rightarrow \Delta^+ + \mu^+ + \mu^- + \Delta^+. \quad (2.4)$$

Only the process (2.1) shown by the diagram (a) was considered so far in the literature.

In the following we will calculate the contributions from the diagrams shown in Fig. 1.

A. Exact $2 \rightarrow 4$ kinematics

In the present studies we perform, for the first time, exact calculations for all the considered exclusive $2 \rightarrow 4$ processes shown in Fig. 1. In general, the cross section can be written as

$$d\sigma = \frac{(2\pi)^4}{2s} |\mathcal{M}_{2 \rightarrow 4}|^2 \frac{d^3 p_1}{(2\pi)^3 2E_1} \frac{d^3 p_2}{(2\pi)^3 2E_2} \frac{d^3 p_3}{(2\pi)^3 2E_3} \frac{d^3 p_4}{(2\pi)^3 2E_4} \times \delta^4(E_a + E_b - p_1 - p_2 - p_3 - p_4). \quad (2.5)$$

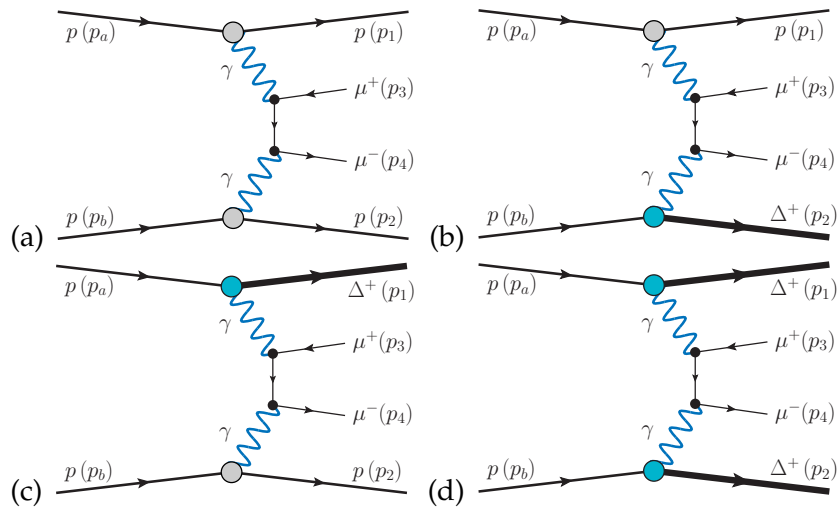


FIG. 1: Diagrams for selected exclusive processes for two-photon production of muon pairs in pp collisions on the Born level. Here only the \hat{t} -channel diagrams are shown. There are also corresponding \hat{u} -channel diagrams with the photon-muon vertices interchanged.

The formula (2.5) is written in the overall center-of-mass frame where energy and momentum conservations have been made explicit, see [11]. The phase space integration variables are taken the same as in [11], except that proton transverse momenta $p_{t,1}$ and $p_{t,2}$ are replaced by $\log_{10}(p_{t,1}/p_{t,0})$ and $\log_{10}(p_{t,2}/p_{t,0})$, $p_{t,0} = 1$ GeV, respectively. In (2.5) $|\mathcal{M}_{2 \rightarrow 4}|^2$ is the $2 \rightarrow 4$ amplitude squared averaged over initial and summed over final particle polarization states. The kinematic variables for the $2 \rightarrow 4$ reaction are

$$s = (p_a + p_b)^2, \quad s_{34} = M_{\mu^+\mu^-}^2 = (p_3 + p_4)^2, \quad (2.6)$$

$$q_1 = p_a - p_1, \quad q_2 = p_b - p_2, \quad t_1 = q_1^2, \quad t_2 = q_2^2; \quad (2.7)$$

$$\hat{p}_t = p_4 - q_2 = q_1 - p_3, \quad \hat{p}_u = q_2 - p_3 = p_4 - q_1, \quad \hat{t} = \hat{p}_t^2, \quad \hat{u} = \hat{p}_u^2,$$

where $p_{a,b}$ and $p_{1,2}$ denote the four-momenta of the baryons, and $p_{3,4}$ denote the four-momenta of the muons, respectively.

The Born amplitudes for the processes (2.1) - (2.4) are calculated as

$$\mathcal{M}_{\lambda_a \lambda_b \rightarrow \lambda_1 \lambda_2 \lambda_3 \lambda_4}(t_1, t_2) = V_{\lambda_a \rightarrow \lambda_1}^{\mu_1}(t_1) \frac{g_{\mu_1 \nu_1}}{t_1} V_{\lambda_3 \lambda_4}^{\nu_1 \nu_2} \frac{g_{\nu_2 \mu_2}}{t_2} V_{\lambda_b \rightarrow \lambda_2}^{\mu_2}(t_2), \quad (2.8)$$

where $\lambda_{a,b}$, $\lambda_{1,2} = \pm \frac{1}{2}$ denote the helicities of the baryons, and $\lambda_{3,4} = \pm \frac{1}{2}$ denote the helicities of the muons, respectively. The $\gamma\gamma \rightarrow \mu^+\mu^-$ interaction includes both \hat{t} - and \hat{u} -channel amplitudes:

$$V_{\lambda_3 \lambda_4}^{\nu_1 \nu_2} = -e^2 \bar{u}(p_4, \lambda_4) \left(\gamma^{\nu_2} \frac{\not{\hat{p}}_t + m_\mu}{\hat{t} - m_\mu^2} \gamma^{\nu_1} + \gamma^{\nu_1} \frac{\not{\hat{p}}_u + m_\mu}{\hat{u} - m_\mu^2} \gamma^{\nu_2} \right) v(p_3, \lambda_3), \quad (2.9)$$

where $\bar{u}(p_4, \lambda_4)$ and $v(p_3, \lambda_3)$ are muon (μ^-) and antimuon (μ^+) spinors, respectively.

The γpp vertex is written as

$$V_{\lambda \rightarrow \lambda'}^{(\gamma pp)^\mu}(p', p) = e \bar{u}(p', \lambda') \left(\gamma^\mu F_1(t) + \frac{i\sigma^{\mu\nu}(p' - p)_\nu}{2m_p} F_2(t) \right) u(p, \lambda), \quad (2.10)$$

where $u(p, \lambda)$ is a Dirac spinor and p, λ and p', λ' are initial and final four-momenta and helicities of the protons, respectively. The form factors $F_1(t)$ and $F_2(t)$ correspond to the proton helicity-conserving and helicity-flipping transitions.

The electromagnetic transition between a proton and spin 1/2 positive parity nucleon resonance N^* , using the Dirac F_1^* and Pauli F_2^* type form factors, satisfying manifestly electromagnetic gauge-invariance, can be written as [26]:

$$V_{\lambda \rightarrow \lambda'}^{(\gamma p N^*)^\mu}(p', p) = e \bar{u}^{(N^*)}(p', \lambda') \left[\left(\gamma^\mu - \frac{(\not{p}' - \not{p})(p' - p)^\mu}{t} \right) F_1^*(t) + \frac{i\sigma^{\mu\nu}(p' - p)_\nu}{m_{N^*} + m_p} F_2^*(t) \right] u(p, \lambda), \quad (2.11)$$

where $u^{(N^*)}$ is the N^* Dirac spinor. The Dirac-type proton-Roper transition form factor $F_1^*(t)$ vanishes at $t = 0$ and stays positive at large $|t|$. On the other hand, the Pauli-type form factor $F_2^*(0) \simeq -0.6$ and changes sign around $-t \simeq 1$ GeV². We take analytic

parametrizations for the electromagnetic $p \rightarrow N^*(1440)$ transition form-factors from [27]; see also Refs. [26, 28–30].

The $\gamma p \Delta$ vertex can be written as [31]

$$V_{\lambda \rightarrow \lambda'}^{(\gamma p \Delta)^\mu}(p', p) = e \bar{u}_\alpha^{(\Delta)}(p', \lambda') \Gamma^{\alpha\mu} u(p, \lambda), \quad (2.12)$$

where

$$\Gamma^{\alpha\mu} = G_M^*(q^2) K_M^{\alpha\mu} + G_E^*(q^2) K_E^{\alpha\mu} + G_C^*(q^2) K_C^{\alpha\mu}, \quad (2.13)$$

in terms of the magnetic dipole G_M^* , electric quadrupole G_E^* , and Coulomb quadrupole G_C^* transition form factors. In (2.12) $u_\alpha^{(\Delta)}$ denotes the Rarita-Schwinger spinor of the spin-3/2 Δ isobar. The $\gamma p \rightarrow \Delta^+$ transition is dominated by the magnetic dipole form factor. We consider therefore only the magnetic transition term with ¹

$$K_M^{\alpha\mu} = \frac{3(m_\Delta + m_p)}{4m_p [(m_\Delta + m_p)^2 - q^2]} \epsilon^{\alpha\mu\rho\sigma} (p' + p)_\rho q_\sigma. \quad (2.14)$$

For the magnetic transition form factor we use the phenomenological parametrization of Ref. [32]

$$G_M^*(q^2) = 3 G_D(q^2) \exp(0.21 q^2) \sqrt{1 - \frac{q^2}{(m_\Delta + m_p)^2}}, \quad (2.15)$$

with the standard dipole form factor $G_D(t) = (1 - t/m_D^2)^{-2}$, $m_D^2 = 0.71 \text{ GeV}^2$. The quality of the parametrization (2.15) was studied in [33].

B. Absorption corrections

The absorptive corrections to the Born amplitude (2.8) are added to give the full physical amplitude for the $pp \rightarrow pp\mu^+\mu^-$ reaction:

$$\mathcal{M}_{pp \rightarrow pp\mu^+\mu^-} = \mathcal{M}_{pp \rightarrow pp\mu^+\mu^-}^{\text{Born}} + \mathcal{M}_{pp \rightarrow pp\mu^+\mu^-}^{\text{absorption}}. \quad (2.16)$$

Here (and above) we have for simplicity omitted the dependence of the amplitude on kinematic variables.

The amplitude including pp -rescattering corrections between the initial- and final-state protons within the one-channel eikonal approach can be written as

$$\mathcal{M}_{pp \rightarrow pp\mu^+\mu^-}^{\text{absorption}}(s, \mathbf{p}_{t,1}, \mathbf{p}_{t,2}) = \frac{i}{8\pi^2 s} \int d^2 \mathbf{k}_t \mathcal{M}_{pp \rightarrow pp}(s, -\mathbf{k}_t^2) \mathcal{M}_{pp \rightarrow pp\mu^+\mu^-}^{\text{Born}}(s, \tilde{\mathbf{p}}_{t,1}, \tilde{\mathbf{p}}_{t,2}), \quad (2.17)$$

where $\tilde{\mathbf{p}}_{t,1} = \mathbf{p}_{t,1} - \mathbf{k}_t$ and $\tilde{\mathbf{p}}_{t,2} = \mathbf{p}_{t,2} + \mathbf{k}_t$. Here, in the overall center-of-mass system, $\mathbf{p}_{t,1}$ and $\mathbf{p}_{t,2}$ are the transverse components of the momenta of the final-state protons and \mathbf{k}_t is

¹ Note that in [31] authors define $q = p' - p$. We have made allowance for this in writing Eq. (2.14).

the transverse momentum carried by additional pomeron exchange. $\mathcal{M}_{pp \rightarrow pp}(s, -\mathbf{k}_t^2)$ is the elastic pp -scattering amplitude for large s and with the momentum transfer $t = -\mathbf{k}_t^2$. We assume s -channel helicity conservation in the pomeron-proton vertices.

In the following we shall show results in the Born approximation as well as when including the absorption corrections on the amplitude level. This allows us to study the absorption effects differentially in any kinematical variable chosen for two-photon induced processes.

C. Equivalent-photon approximation

In the collinear EPA approach, with neglected photon transverse momenta, one can write the differential cross section as

$$\frac{d\sigma}{dy_3 dy_4 d^2\mathbf{p}_{t,\mu}} = \frac{1}{16\pi^2 \hat{s}^2} x_1 f(x_1) x_2 f(x_2) \overline{|\mathcal{M}_{\gamma\gamma \rightarrow \mu^+\mu^-}|^2}, \quad (2.18)$$

where $\hat{s} = sx_1x_2$. $f(x)$'s are elastic fluxes of the equivalent photons as a function of longitudinal momentum fraction with respect to the parent proton defined by the kinematical variables of the muons,

$$\begin{aligned} x_1 &= \frac{m_{t,3}}{\sqrt{s}} \exp(y_3) + \frac{m_{t,4}}{\sqrt{s}} \exp(y_4), \\ x_2 &= \frac{m_{t,3}}{\sqrt{s}} \exp(-y_3) + \frac{m_{t,4}}{\sqrt{s}} \exp(-y_4), \end{aligned} \quad (2.19)$$

where $m_{t,\mu} = \sqrt{|\mathbf{p}_{t,\mu}|^2 + m_\mu^2}$. In (2.18) $\overline{|\mathcal{M}|^2}$ is the $\gamma\gamma \rightarrow \mu^+\mu^-$ amplitude squared averaged over the photon and summed over the muon polarization states. For the elastic photon fluxes $f(x)$ we take the formulas given in [34], see [7]. The photon fluxes associated with Δ production are taken from Ref. [17].

D. k_t -factorization approach

In the recent k_t -factorization approach [20, 21] the differential cross section for the $pp \rightarrow X\mu^+\mu^-Y$ reaction (X and Y represent the hadronic systems resulting from the proton dissociation) can be written as

$$\begin{aligned} \frac{d\sigma(pp \rightarrow X\mu^+\mu^-Y)}{dy_3 dy_4 d^2\mathbf{p}_{t,3} d^2\mathbf{p}_{t,4} dM_X dM_Y} &= \frac{1}{16\pi^2 \hat{s}^2} \int \frac{d^2\mathbf{q}_{t,1}}{\pi q_{t,1}^2} \frac{d^2\mathbf{q}_{t,2}}{\pi q_{t,2}^2} x_1 \frac{d\gamma(x_1, \mathbf{q}_{t,1}, M_X)}{dM_X} x_2 \frac{d\gamma(x_2, \mathbf{q}_{t,2}, M_Y)}{dM_Y} \\ &\times \sum_{\lambda_3 \lambda_4} |M(\lambda_3, \lambda_4; \mathbf{q}_{t,1}, \mathbf{q}_{t,2})|^2 \delta^{(2)}(\mathbf{q}_{t,1} + \mathbf{q}_{t,2} - \mathbf{p}_{t,3} - \mathbf{p}_{t,4}). \end{aligned} \quad (2.20)$$

Here $\mathbf{q}_{t,1}$ and $\mathbf{q}_{t,2}$ are the transverse momentum vectors of virtual photons. The inelastic photon fluxes, $\gamma(x_1, \mathbf{q}_{t,1}, M_X)$ and $\gamma(x_2, \mathbf{q}_{t,2}, M_Y)$, are expressed in terms of deep-inelastic structure functions [21] known from many experiments. Different parametrizations were proposed in the literature (see e.g. [21] and references therein).

III. RESULTS

A. Exact $2 \rightarrow 4$ approach

In calculating the cross section of the photon initiated dimuon production we perform integration in auxiliary variables $\log_{10}(p_{t,1}/1 \text{ GeV})$ and $\log_{10}(p_{t,2}/1 \text{ GeV})$ instead of the outgoing baryon's transverse momenta ($p_{t,1}$ and $p_{t,2}$) as usually done. The differential distribution $d\sigma/d[\log_{10}(p_{t,1}/1 \text{ GeV})]$ is shown in the panel (a) of Fig. 2 for the ATLAS kinematics ($\sqrt{s} = 13 \text{ TeV}$, $|\eta_\mu| < 2.5$, $p_{t,\mu} > 6 \text{ GeV}$, $M_{\mu^+\mu^-} \in (12, 30) \text{ GeV}$). Results for the $pp \rightarrow pp\mu^+\mu^-$ reaction (2.1) are shown by the black solid lines. Results for the reactions (2.2) - (2.4) with $\Delta(1232)$ isobars in the final state are shown by the red dashed lines. The blue dotted lines correspond to the contributions with production of the Roper resonance $N^* \equiv N(1440)$. In the panel (b) of Fig. 2 we present distribution in transferred four-momentum squared t_1 between the initial and final baryons. The distributions in $\log_{10}(p_{t,2}/1 \text{ GeV})$ and $|t_2|$ are the same as those from the panel (a) and (b), respectively, but with a different component designations $\Delta p \leftrightarrow p\Delta$ and $N^*p \leftrightarrow pN^*$. We find that from the side of $p \rightarrow \Delta(1232)$ and $p \rightarrow N(1440)$ transitions the differential cross sections $d\sigma/d|t|$ vanish when $|t| \rightarrow 0$.

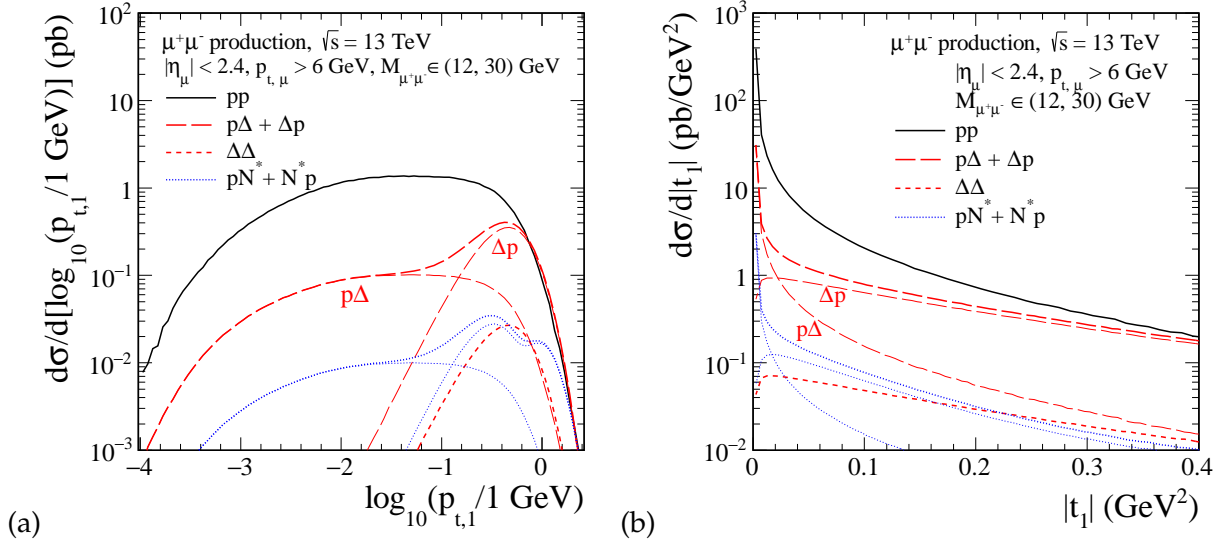


FIG. 2: The differential cross sections $d\sigma/d[\log_{10}(p_{t,1}/1 \text{ GeV})]$ (panel (a)), and $d\sigma/d|t_1|$ (panel (b)) for various exclusive processes of the $\mu^+\mu^-$ production at $\sqrt{s} = 13 \text{ TeV}$ and for the ATLAS experimental cuts. No absorption effects were taken into account here.

In Fig. 3 we present differential observables for the recent ATLAS experimental cuts [1]. In the panel (a) we show $\mu^+\mu^-$ invariant mass distributions for the reactions (2.2) - (2.4). Here the horizontal error bars mean just bin width. We see that the $pp \rightarrow pp\mu^+\mu^-$ contribution alone (see the black solid line) exceeds the ATLAS data from [1]. As we will show below this is also true when including the absorptive corrections in our calculations, see Fig. 7. Inclusion of exclusive channels with $\Delta(1232)$ and $N(1440)$ resonances increases further the cross section for $\mu^+\mu^-$ production. In the panel (b) we show distribution in the modulus of sum of the transverse momentum vectors of muons $p_{t,\mu^+\mu^-} = |\mathbf{p}_{t,\mu^+\mu^-}|$, $\mathbf{p}_{t,\mu^+\mu^-} = \mathbf{p}_{t,\mu^+} + \mathbf{p}_{t,\mu^-}$. For the contributions with Δ and $N(1440)$

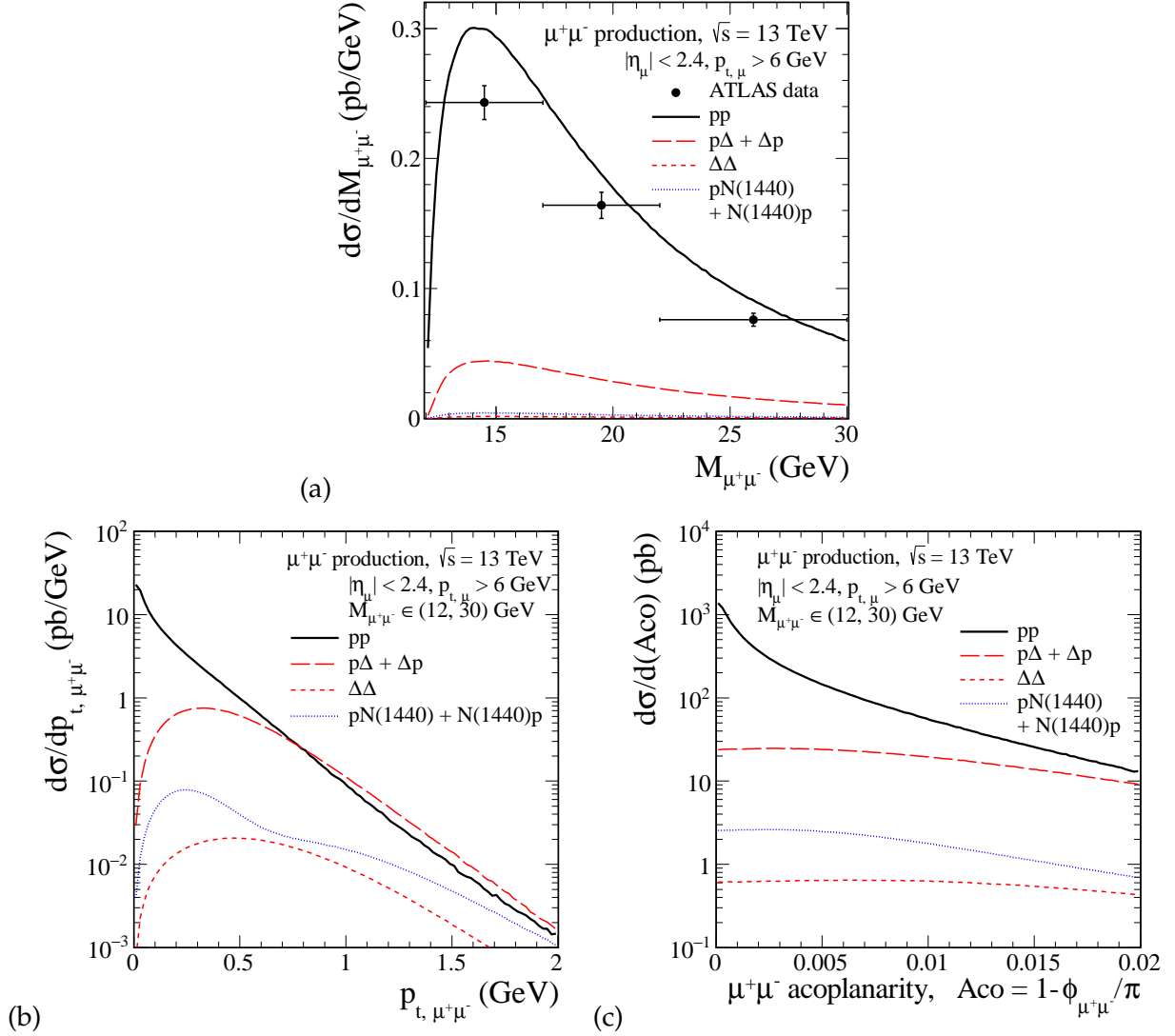


FIG. 3: The differential cross sections for various exclusive processes (2.1) - (2.4) specified in the figure legend for the $\mu^+\mu^-$ production in pp collisions. Calculations are done for $\sqrt{s} = 13$ TeV, $|\eta_\mu| < 2.5$, $p_{t,\mu} > 6$ GeV, and in dimuon invariant mass region $M_{\mu^+\mu^-} \in (12, 30)$ GeV. No absorption effects are taken into account here. The ATLAS experimental data from [1] are shown for comparison (see panel (a)).

resonances the cross section $d\sigma/dp_{t,\mu^+\mu^-}$ vanishes when $p_{t,\mu^+\mu^-} \rightarrow 0$. The ATLAS experiment imposes a cut on $p_{t,\mu^+\mu^-} < 1.5$ GeV (see Fig. 2 (d) in [1]). We can see that such a cut practically does not influence the cross section. The relative contribution of resonance production increases with $p_{t,\mu^+\mu^-}$ and can be even bigger than for the $pp \rightarrow pp\mu^+\mu^-$ contribution. The panel (c) shows the distribution in the dimuon acoplanarity variable defined by $Aco = 1 - \phi_{\mu^+\mu^-}/\pi$, where $\phi_{\mu^+\mu^-}$ is azimuthal angle between the muons. Rather different acoplanarity distributions are obtained for the different processes considered here. However, no acoplanarity cut is imposed by the recent ATLAS experiment.

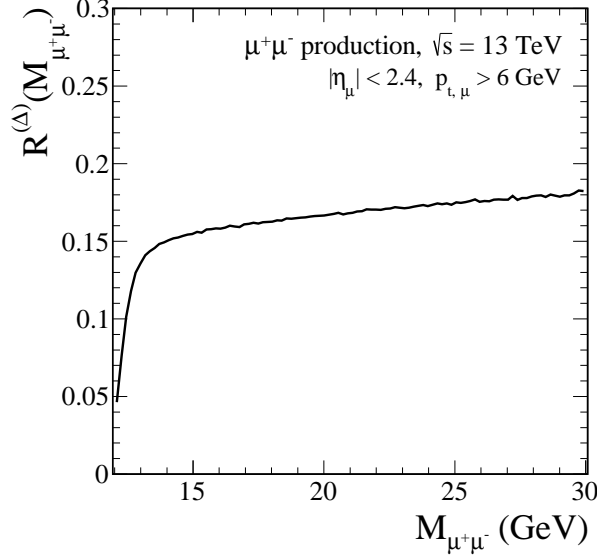


FIG. 4: The ratio $R^{(\Delta)}(M_{\mu^+\mu^-})$ defined by Eq.(3.1) for the $\mu^+\mu^-$ production at $\sqrt{s} = 13$ TeV and for the ATLAS cuts.

In Fig. 4 we show the ratio

$$R^{(\Delta)}(M_{\mu^+\mu^-}) = \frac{d\sigma^{(p\Delta)}/dM_{\mu^+\mu^-} + d\sigma^{(\Delta p)}/dM_{\mu^+\mu^-} + d\sigma^{(\Delta\Delta)}/dM_{\mu^+\mu^-}}{d\sigma^{(pp)}/dM_{\mu^+\mu^-}} \quad (3.1)$$

for $\sqrt{s} = 13$ TeV and the ATLAS experimental cuts. In (3.1), e.g., $d\sigma^{(p\Delta)}/dM_{\mu^+\mu^-}$ is the differential cross section for the $pp \rightarrow p\mu^+\mu^-\Delta^+$ reaction (2.2). The contribution of the new processes (2.2) - (2.4) increases with increasing $M_{\mu^+\mu^-}$. The ratio exceeds 15% for $M_{\mu^+\mu^-} > 14$ GeV.

So far we have omitted effect related to extra soft interactions which lead to a reduction of the cross section with the extra requirement of rapidity gap. How big is effect of the absorption associated with different exclusive effects? Is it the same for different components? These questions are very important but go beyond the scope of the present paper.

In Fig. 5 we show the relative effect of absorption, for the $pp \rightarrow pp\mu^+\mu^-$ reaction,

$$\langle S^2(x) \rangle = \frac{d\sigma^{\text{absorption}}/dx}{d\sigma^{\text{Born}}/dx}, \quad (3.2)$$

where $x = M_{\mu^+\mu^-}, p_{t,\mu^+\mu^-}, \text{Aco}$. In (3.2) $d\sigma^{\text{absorption}}/dx$ is the differential cross section including the absorptive effects at the amplitude level as described in Sec. II B and $d\sigma^{\text{Born}}/dx$ is the differential cross section without the absorption. We predict somewhat larger absorption for the pN^*, N^*p , and N^*N^* contributions than for the traditional pp final state (not shown here). Our calculations suggest similar effect for the $p\Delta, \Delta p$, and $\Delta\Delta$ final states for which explicit calculation is rather difficult. The effect of the absorption depends on kinematics but is rather small. The effect would increase somewhat when adding intermediate proton resonance states. Such a calculation is more difficult and requires input, $pN^*\mathbb{P}$, $pN^*\gamma$ couplings, which is not available at present.

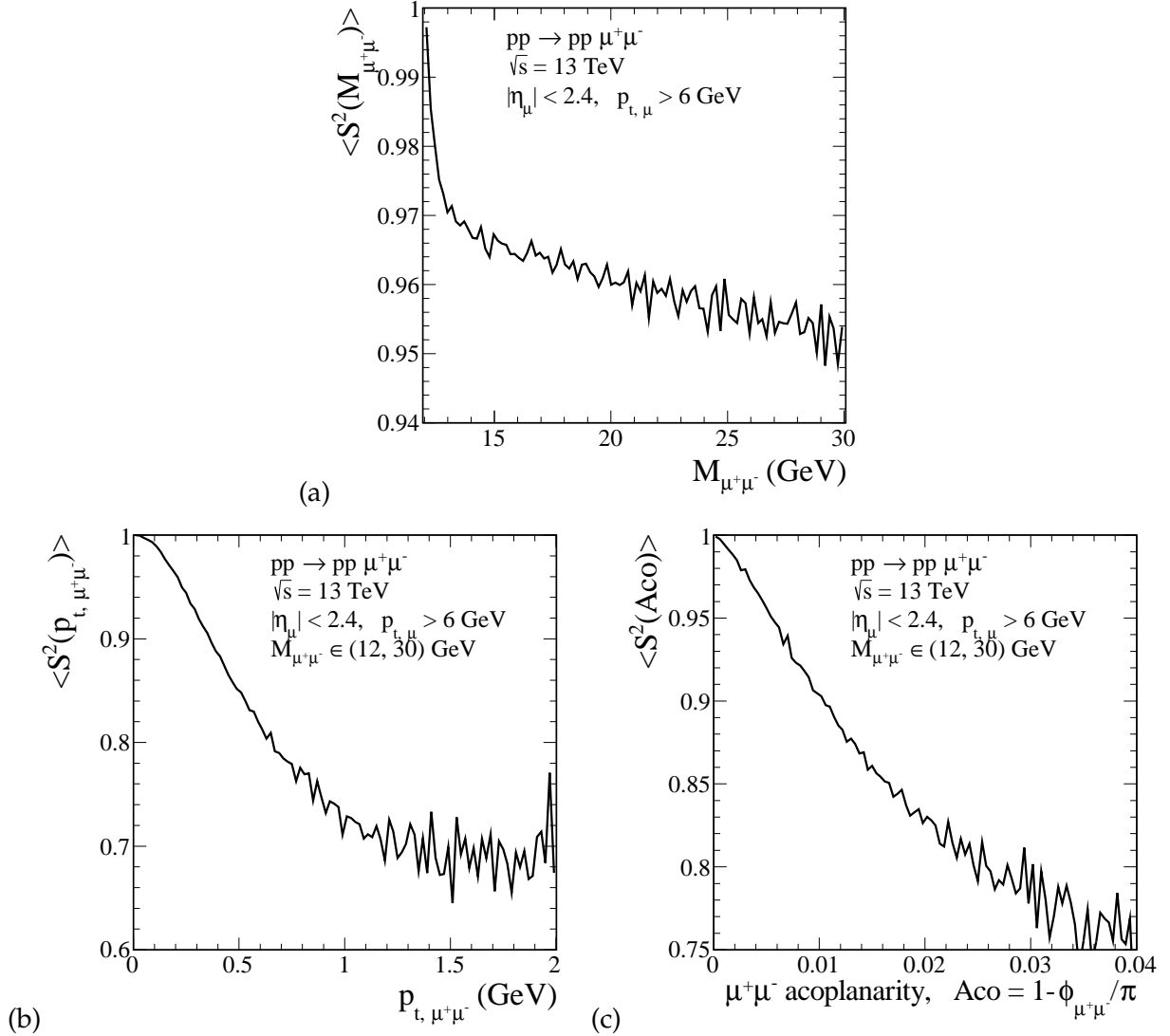


FIG. 5: The ratios $\langle S^2 \rangle$ (3.2) as a function of $M_{\mu^+\mu^-}$ (panel (a)), $p_{t,\mu^+\mu^-}$ (panel (b)), dimuon acoplanarity (panel (c)). Calculations were done at $\sqrt{s} = 13$ TeV and for the ATLAS cuts.

B. k_t -factorization approach

In this subsection we wish to show the differential distributions obtained in the k_t -factorization approach. The results of the single or double dissociative processes enter the cross section via so-called deep-inelastic structure functions. In our calculation we have used two different parametrizations of the proton structure function $F_2(x, Q^2)$ taken from the literature: (1) Fiore *et al.* parametrization [35, 36] (labeled by us FFJLM) based on a Regge-dual model that explicitly includes the prominent nucleon resonances plus a smooth background to describe the F_2 experimental data for $p(e, e')X$ reaction measured at the JLab; and (2) Szczurek-Uleshchenko (SU) parametrization [37] which gives good description at rather small and intermediate Q^2 at not too small x .

In Fig. 6 we compare different distributions ($d\sigma/dM_{\mu^+\mu^-}$, $d\sigma/dp_{t,\mu^+\mu^-}$, $d\sigma/d\phi_{\mu^+\mu^-}$) for purely elastic (the solid line), single dissociative (the dashed line), and double disso-

ciative (the dotted line) contributions. In the calculations we have included all cuts of the ATLAS experiment [1], including also the cut on $p_{t,\mu^+\mu^-} < 1.5$ GeV. Results for the continuum dissociative contributions (labeled as SU) were calculated using the Szczurek-Uleshchenko parametrization of F_2 experimental data. The shapes of the $M_{\mu^+\mu^-}$ distributions (see the panel (a)) are very similar while the other distributions are rather different. In the panel (b) we present in addition results for resonance production obtained in the FFJLM parametrization; see the red lines (labeled as FFJLM). Here $pR + Rp$ denotes contribution when three resonances $\Delta(1232) \frac{3}{2}^+$, $N^*(1520) \frac{3}{2}^-$, and $N^*(1680) \frac{5}{2}^+$ are added together. For comparison, we show also the result with only $\Delta(1232)$ resonances ($p\Delta + \Delta p$ component). One can explicitly see that the cut on $p_{t,\mu^+\mu^-}$ reduces the dissociative contributions (see also Table I). No cut on $\phi_{\mu^+\mu^-}$ was imposed in the ATLAS experiment. But it should be realized that such a cut is strongly correlated with the cut on $p_{t,\mu^+\mu^-}$ (compare the black and blue lines in the panel (c)).

We remind that the ATLAS collaboration imposes extra condition on $p_{t,\mu^+\mu^-} < 1.5$ GeV [1]. Inclusion of such a cut suppresses the relative amount of dissociative continuum contributions but definitely does not solve the problem of the need of large absorption effects. A large size of the dissociation into continuum requires a special comment. At large $p_{t,\mu^+\mu^-}$ the single and double continuum dissociative processes should dominate. As shown recently in [38] the absorption effect for $\sqrt{s} = 13$ TeV and $M_X, M_Y < 50$ GeV associated with remnant fragmentation(s) are rather small. So far other absorption effects were not calculated consistently in the literature.

At present ATLAS collaboration used some procedure to reduce the background from the single and double dissociation processes (see Sec. 5 of [1]). However, this procedure may be model dependent and in our opinion requires further studies. It would be valuable to confront the extracted contribution with our model calculation. Also absorption effects for the continuum dissociation are not fully understood in our opinion.

C. Cross sections and comparison with the ATLAS experimental data

The ATLAS collaboration has measured the fiducial cross section of the $pp \rightarrow pp\mu^+\mu^-$ reaction at $\sqrt{s} = 13$ TeV [1]. The experimental result is

$$\sigma_{\text{exp., fid.}}(pp \rightarrow pp\mu^+\mu^-) = 3.12 \pm 0.07 \text{ (stat.)} \pm 0.14 \text{ (syst.) pb}, \quad (3.3)$$

for both dimuon invariant mass ranges and for $p_{t,\mu}$ and $|\eta_\mu|$ requirements:

$$12 \text{ GeV} < M_{\mu^+\mu^-} < 30 \text{ GeV}, \quad p_{t,\mu} > 6 \text{ GeV}, \quad |\eta_\mu| < 2.4, \quad (3.4)$$

$$30 \text{ GeV} < M_{\mu^+\mu^-} < 70 \text{ GeV}, \quad p_{t,\mu} > 10 \text{ GeV}, \quad |\eta_\mu| < 2.4. \quad (3.5)$$

The sum of cross sections calculated within the “exact $2 \rightarrow 4$ approach” (see Sec. II A) for the experimental cuts (3.4) and (3.5), respectively, is found to be

$$\sigma_{\text{exact}}^{(\text{Born})}(pp \rightarrow pp\mu^+\mu^-) = 3.01 \text{ pb} + 0.55 \text{ pb} = 3.56 \text{ pb} \quad (3.6)$$

without the absorptive corrections, and

$$\sigma_{\text{exact}}^{(\text{absorption})}(pp \rightarrow pp\mu^+\mu^-) = 2.89 \text{ pb} + 0.51 \text{ pb} = 3.40 \text{ pb} \quad (3.7)$$

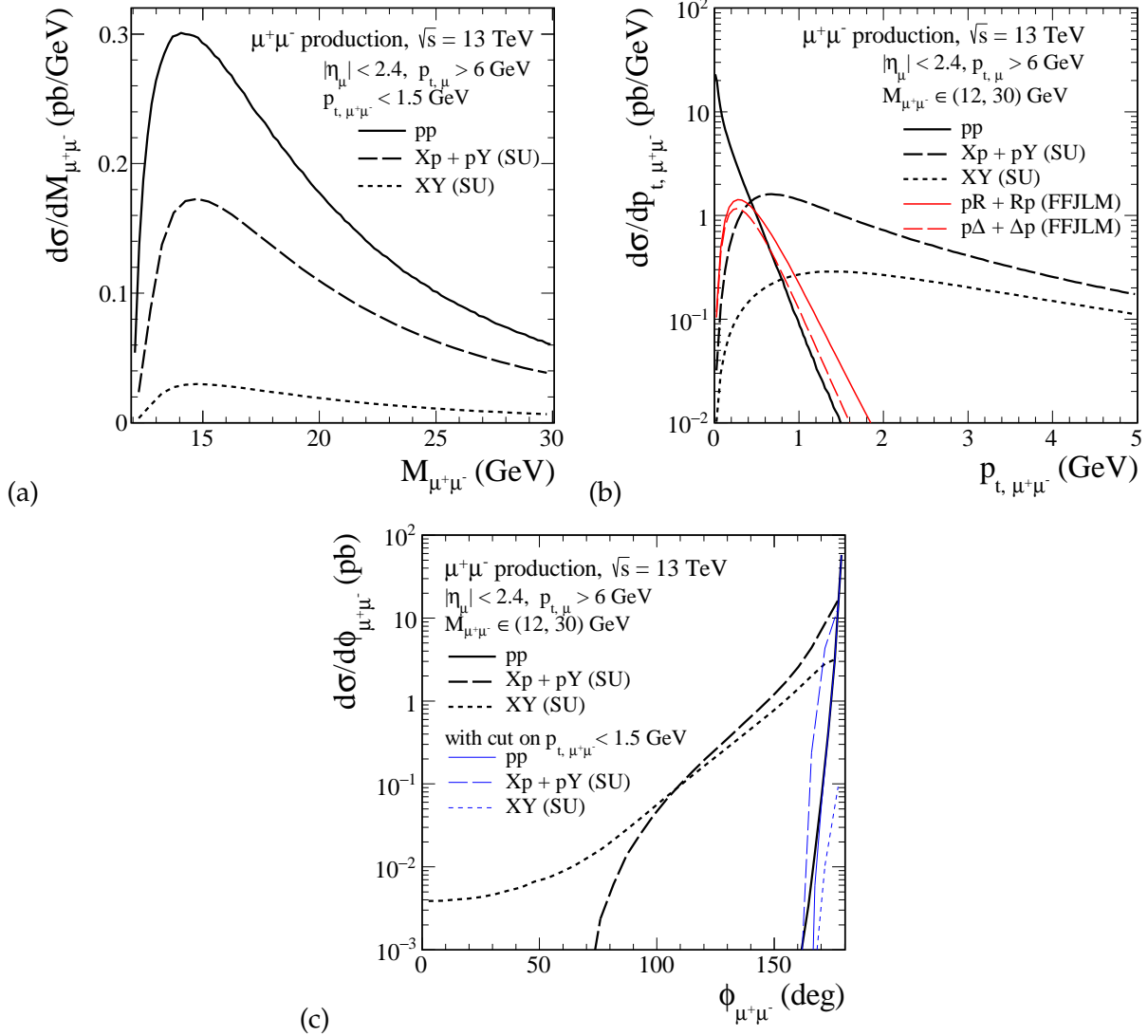


FIG. 6: Single and double dissociative continuum contributions for $d\sigma/dM_{\mu^+\mu^-}$ (panel (a)), $d\sigma/dp_{T,\mu^+\mu^-}$ (panel (b)), and $d\sigma/d\phi_{\mu^+\mu^-}$ (panel (c)) obtained within the k_t -factorization approach for the recent ATLAS experimental cuts [1]. For the continuum processes the Szczurek-Uleshchenko parametrization (labeled as SU) was used in the calculation and we impose an upper limit on dissociative systems $M_X, M_Y < 50$ GeV. For comparison, the solid lines represent the results for the purely elastic contribution (2.1). In the panel (b) also the results for resonant contributions (labeled as FFJLM) are shown. In the panel (c) the black lines correspond to the results without the cut on $p_{T,\mu^+\mu^-}$. The blue lines show results obtained including all experimental cuts.

including the absorptive corrections as discussed in Sec. II B.

The authors of [1] compare their result (3.3) with the theoretical predictions of two models with absorptive corrections. Our result (3.7) is in good agreement with the SuperChic MC [39] result $\sigma = 3.45 \pm 0.05$ pb quoted in [1]. However, smaller cross section was obtained in the finite-size EPA approach [9] that gives $\sigma = 3.06 \pm 0.05$ pb.

In Fig. 7 we present the dimuon invariant mass distributions for our “exact $2 \rightarrow 4$ kinematics” approach for the $pp \rightarrow pp\mu^+\mu^-$ process, without (the blue dashed lines)

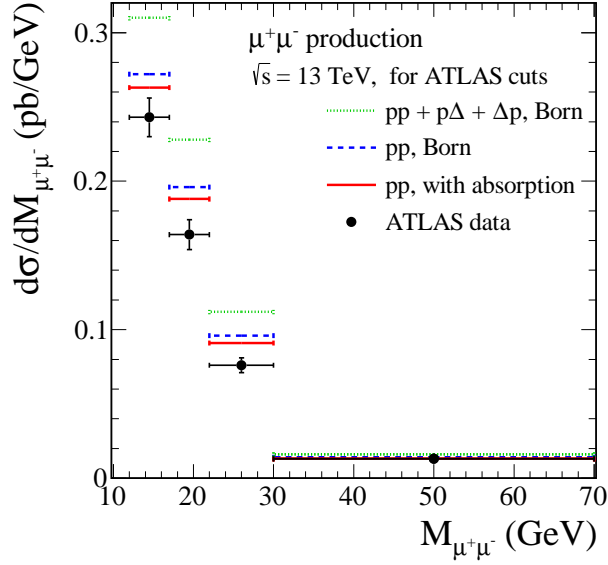


FIG. 7: The differential cross sections $d\sigma/dM_{\mu^+\mu^-}$ for the $\mu^+\mu^-$ production at $\sqrt{s} = 13$ TeV with the ATLAS experimental cuts specified in (3.4) and (3.5). Our “exact $2 \rightarrow 4$ kinematics” predictions (lines) are compared with the ATLAS differential fiducial cross sections from Table 3 of [1]. The green-dotted lines and blue-dashed lines represent the Born results for the $pp \rightarrow pp\mu^+\mu^-$ plus that for the $pp \rightarrow p\Delta\mu^+\mu^-$ ($\Delta p\mu^+\mu^-$) processes and for the $pp \rightarrow pp\mu^+\mu^-$ process alone, respectively. The red solid bottom lines represent the results for the $pp \rightarrow pp\mu^+\mu^-$ reaction with the absorptive effects included.

and with (the red solid lines) absorption effects together with the ATLAS results from Table 3 of [1]. For the $pp \rightarrow pp\mu^+\mu^-$ component we get the theoretical survival factor values $\langle S^2 \rangle = \sigma_{\text{exact}}^{(\text{absorption})} / \sigma_{\text{exact}}^{(\text{Born})} = 0.97, 0.96, 0.95$, and 0.93 integrated according to the four experimental bins, respectively. For comparison we need $0.92, 0.87, 0.84$, and 1.00 to describe the ATLAS data. Larger suppression factors are necessary to describe the ATLAS data especially when taking into account contributions with Δ isobars in the final state: $0.78, 0.72, 0.68$, and 0.81 , respectively. These numbers are far from unity often naively expected for two-photon exclusive processes. In general, the absorption effects may depend on the final state. Here we have presented our estimates for the $pp \rightarrow pp\mu^+\mu^-$ process. As already discussed, it is very difficult to make similar predictions for the $pp \rightarrow p\Delta\mu^+\mu^-$ or $pp \rightarrow \Delta p\mu^+\mu^-$ processes. A comparison with experimental data suggests that the corresponding effects should be much bigger than for the $pp \rightarrow pp\mu^+\mu^-$ process.

In Table I we have collected integrated cross sections for different contributions calculated in three different approaches: exact $2 \rightarrow 4$ (see Secs. II A and II B), EPA (see Sec. II C), and k_t -factorization (see Sec. II D). Results for experimental cuts $|\eta_\mu| < 2.4$, $p_{t,\mu}$, $M_{\mu^+\mu^-}$, and $p_{t,\mu^+\mu^-}$ are shown. The results obtained within the exact $2 \rightarrow 4$ approach imposing the ATLAS cuts (3.4) are similar to the results obtained within the EPA approach. We get a slightly larger cross section for the $pp \rightarrow pp\mu^+\mu^-$ process within the k_t -factorization approach. There are also results for the single and double resonance production (FFJLM parametrization [35]) and dissociative continuum contributions (SU

TABLE I: Cross sections for different processes for central exclusive production of $\mu^+\mu^-$ pairs calculated for three different approaches. The calculations was performed for $\sqrt{s} = 13$ TeV and with different experimental cuts. In the k_t -factorization approach for the continuum processes (labeled as SU) we take an upper limit on M_X and $M_Y < 50$ GeV. In the case of resonance production (FFJLM) R means processes when contributions of three resonances $\Delta(1232)$, $N^*(1520)$, and $N^*(1680)$ are added together. No absorption effects were included here.

$ \eta_\mu < 2.4$	Y	Y	Y	Y
$p_{t,\mu} > 6$ GeV		Y	Y	Y
$12 < M_{\mu^+\mu^-} < 30$ GeV			Y	Y
$p_{t,\mu^+\mu^-} < 1.5$ GeV				Y
Exact $2 \rightarrow 4$ approach	σ (nb)	σ (pb)	σ (pb)	σ (pb)
$pp \rightarrow pp\mu^+\mu^-$	32.56	3.81	3.01	3.01
$pp \rightarrow p\Delta\mu^+\mu^-$	0.67	0.31	0.23	0.23
$pp \rightarrow \Delta p\mu^+\mu^-$	0.67	0.31	0.23	0.23
$pp \rightarrow \Delta\Delta\mu^+\mu^-$	0.02	0.02	0.02	0.02
EPA				
$pp \rightarrow pp\mu^+\mu^-$	37.08	3.68	2.97	
$pp \rightarrow p\Delta\mu^+\mu^-$	1.87	0.33	0.26	
$pp \rightarrow \Delta p\mu^+\mu^-$	1.87	0.33	0.26	
$pp \rightarrow \Delta\Delta\mu^+\mu^-$	0.09	0.03	0.02	
k_t-factorization approach				
$pp \rightarrow pp\mu^+\mu^-$	39.74	3.91	3.16	
$pp \rightarrow p\Delta\mu^+\mu^-$ (FFJLM)	1.33	0.41	0.32	
$pp \rightarrow \Delta p\mu^+\mu^-$ (FFJLM)	1.33	0.41	0.32	
$pp \rightarrow \Delta\Delta\mu^+\mu^-$ (FFJLM)	0.02	0.01		
$pp \rightarrow pR\mu^+\mu^-$ (FFJLM)	1.65	0.55	0.43	
$pp \rightarrow Rp\mu^+\mu^-$ (FFJLM)	1.65	0.55	0.43	
$pp \rightarrow RR\mu^+\mu^-$ (FFJLM)	0.03	0.02		
$pp \rightarrow pY\mu^+\mu^-$ (SU)		2.38	1.84	0.88
$pp \rightarrow Xp\mu^+\mu^-$ (SU)		2.38	1.84	0.88
$pp \rightarrow XY\mu^+\mu^-$ (SU)		1.76	1.32	0.30

parametrization [37]) calculated within the k_t -factorization approach. The resonance production constitutes about 20% of the fully exclusive $pp \rightarrow pp\mu^+\mu^-$ contribution, that is, somewhat larger than from our $2 \rightarrow 4$ calculation without absorption effects. The double resonance contribution is less than 1% of the purely exclusive component and can be in practice neglected. The contributions of single and double dissociation continuum with all the cuts described in Table I constitute 68% of the purely exclusive component but was hopefully removed by the ATLAS extraction procedure [1]. These are non-negligible contributions, larger than typical size of absorption effects for the $pp \rightarrow pp\mu^+\mu^-$ process.

We have much larger problem of overestimating the ATLAS experimental data than signaled in [1], see also Fig. 7. This probably means that the continuum contributions

are subjected to much larger absorption effects than contributions with resonances in the final state. This is very interesting problem but clearly goes beyond the scope of the present paper, where we have focused mainly on the contributions with resonances in the final state. Solving the problem requires probably inclusion of multi-parton processes [40] and remnant fragmentation [41]. The parameters of the multi-parton interactions were adjusted rather to gg induced processes and cannot be used for our $\gamma\gamma$ induced processes. Recently, in Ref. [38], the effect of rapidity gap survival factor associated with remnant fragmentation was studied for W^+W^- production. Such effects strongly depend on details of experiment. The effects of absorption were of course not included by the ATLAS collaboration when “subtracting” the dissociative contributions.

D. Predictions for ATLAS + ALFA experiment

The measurement of forward protons would be useful in our opinion to better understand absorption effects. There are several efforts to complete installation of forward proton detectors. The CMS collaboration combines efforts with the TOTEM collaboration while the ATLAS collaboration may use the ALFA sub-detectors.

Here we wish to show our predictions for $\sqrt{s} = 13$ TeV based on the exact $2 \rightarrow 4$ approach (see Sec. II A) including the ATLAS experimental cuts (3.4) and with extra cuts on the leading protons of $0.17 \text{ GeV} < |p_{y,1}|, |p_{y,2}| < 0.5 \text{ GeV}$ [42] as will be the proton momentum window for ALFA detectors on both sides of the ATLAS detector.

We obtain the Born cross section

$$\sigma_{\text{exact}}^{(\text{Born})}(pp \rightarrow pp\mu^+\mu^-) = 12.87 \text{ fb} + 12.12 \text{ fb} = 24.99 \text{ fb} \quad (3.8)$$

and including the absorptive corrections (see Sec. II B)

$$\sigma_{\text{exact}}^{(\text{absorption})}(pp \rightarrow pp\mu^+\mu^-) = 11.32 \text{ fb} + 2.56 \text{ fb} = 13.88 \text{ fb}. \quad (3.9)$$

In (3.8) and (3.9) we sum resulting cross sections for two exclusive conditions $p_{y,1}p_{y,2} < 0$ and $p_{y,1}p_{y,2} \geq 0$. We obtain much bigger reduction of the cross section due to absorption effects when $p_{y,1}p_{y,2} \geq 0$.

In Fig. 8 we present distributions in some observables with the ATLAS + ALFA experimental cuts without (the blue thin lines) and with (the black thick lines) absorption effects. Results for two conditions $p_{y,1}p_{y,2} < 0$ (the long-dashed lines) and $p_{y,1}p_{y,2} \geq 0$ (the dotted lines) and their sum (the solid lines) are shown. Inclusion of absorption effects modifies the differential distributions because their shapes depend on the kinematics of outgoing protons. The measurement of such distributions would allow us to better understand absorption effects.

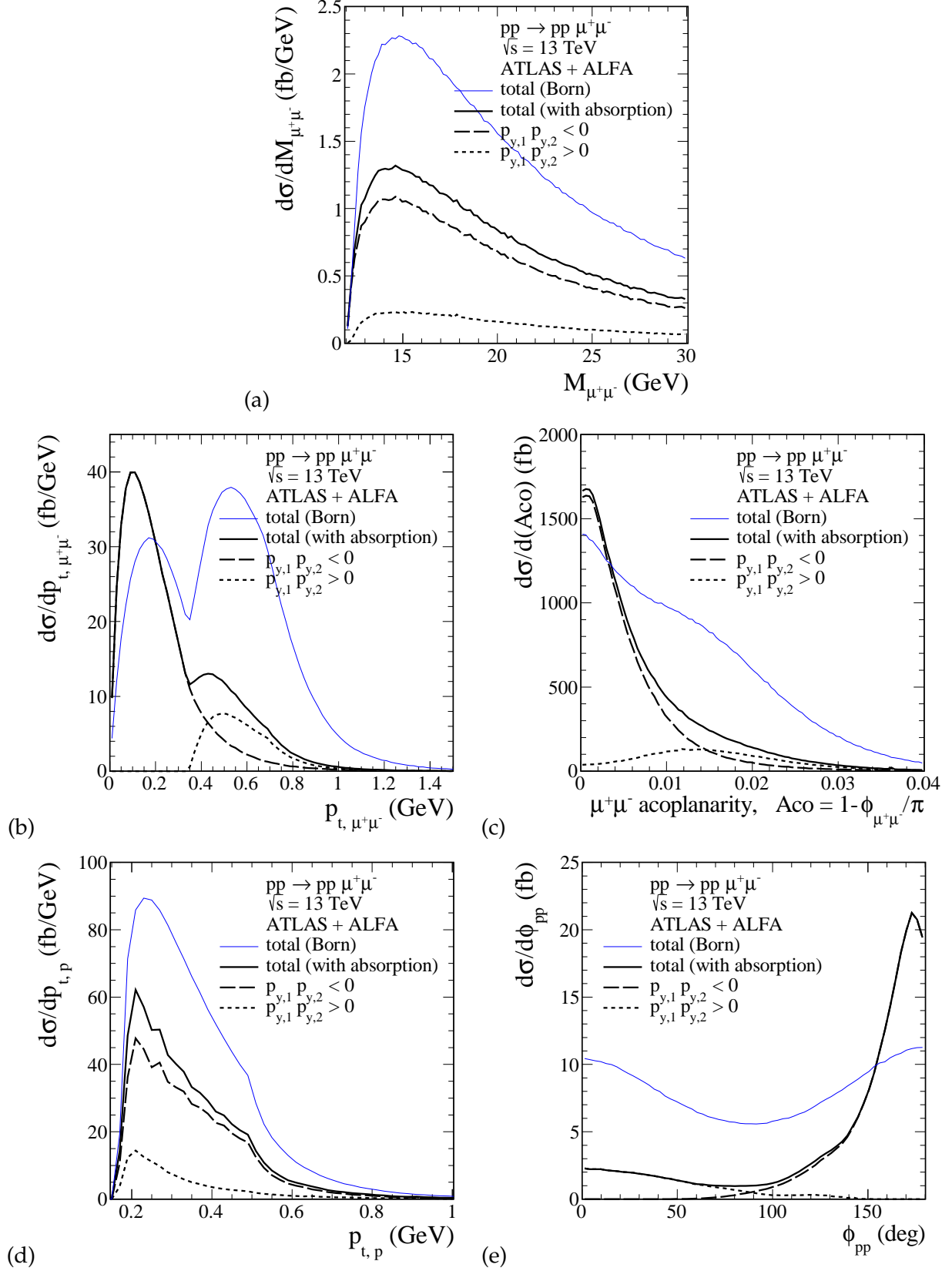


FIG. 8: The differential cross sections for the $pp \rightarrow pp \mu^+ \mu^-$ reactions for $\sqrt{s} = 13 \text{ TeV}$ and ATLAS + ALFA experimental cuts. The blue thin lines correspond to the Born results while the black thick lines correspond to the results with absorption effects included.

IV. CONCLUSIONS

In the present paper we have explicitly calculated contribution of the $pp \rightarrow p\Delta\mu^+\mu^-$ and $pp \rightarrow \Delta\Delta\mu^+\mu^-$ processes both in momentum space EPA (using associated photon fluxes derived earlier) and in exact kinematically $2 \rightarrow 4$ calculation. We have considered similar contributions for the Roper resonance ($N(1440)$). For comparison we have shown also results of calculation obtained within the k_t -factorization approach. Using some parametrizations from the literature of the proton structure functions one can include also contributions with proton resonances in the final state. Also contributions with single and double continuum dissociation have been obtained in this way and have been shown for comparison.

The resonance contributions constitute about 15% of the conventional $pp \rightarrow pp\mu^+\mu^-$ cross section and leads to an enhancement over the measured recently cross sections when ignoring absorption effects. The resulting cross sections from the k_t -factorization approach are somewhat larger as those obtained in the explicit $2 \rightarrow 4$ calculation.

The $2 \rightarrow 4$ calculation allows to include absorption effects on the amplitude level. The absorption effects lead to a damping of the cross section. The effect depends on the collision energy and kinematical variables. The corresponding results have been quantified. However, we have checked numerically that the effect of absorption for the contributions with one or two $N(1440)$ resonance is larger than for the conventional $pp \rightarrow pp\mu^+\mu^-$ one. Our calculations suggest similar effect for the processes with Δ resonance production. But even for the dominant $pp \rightarrow pp\mu^+\mu^-$ process the resulting cross section overestimate the ATLAS experimental data.

We have shown that in the final comparison with experimental data one should also take into account contributions when one or both protons dissociate into continuum. Naive adding of such contributions would lead to clear overestimation of the measured cross sections. Rapidity gap survival factor associated with remnant fragmentation seems highly insufficient, see Ref. [38]. Clearly some absorption effects are missing. Multi-parton interactions (see, e.g., Ref. [40]) are obvious candidates but it is not clear how to include them in a consistent manner. The parameters of the multi-parton interactions are usually adjusted to processes initiated by two gluons but not two photons, so cannot be directly used in our case. In our opinion the new experimental data should trigger further studies.

To meet the expectations of the experimental measurement with dedicated forward detectors we have estimated the cross section for the ATLAS and ALFA experimental cuts. The cross section for the purely exclusive $pp \rightarrow pp\mu^+\mu^-$ reaction, taking into account absorption effects, is of order of 0.01 pb (3.9). Several differential distributions have been presented. We have shown only results for purely non-resonant exclusive component. What is the role of other semiexclusive processes considered here will require further experimental and theoretical studies.

Acknowledgments

We are indebted to Leszek Adamczyk, Wolfgang Schäfer and Rafał Staszewski for useful discussions. This research was partially supported by the Polish National Science Centre Grant No. 2014/15/B/ST2/02528 and by the Centre for Innovation and Transfer

- [1] M. Aaboud *et al.*, (ATLAS Collaboration), *Measurement of the exclusive $\gamma\gamma \rightarrow \mu^+\mu^-$ process in proton-proton collisions at $\sqrt{s} = 13$ TeV with the ATLAS detector*, Phys. Lett. **B777** (2018) 303, arXiv:1708.04053 [hep-ex].
- [2] S. Chatrchyan *et al.*, (CMS Collaboration), *Exclusive $\gamma\gamma \rightarrow \mu^+\mu^-$ production in proton-proton collisions at $\sqrt{s} = 7$ TeV*, JHEP **01** (2012) 052, arXiv:1111.5536 [hep-ex].
- [3] S. Chatrchyan *et al.*, (CMS Collaboration), *Search for exclusive or semi-exclusive $\gamma\gamma$ production and observation of exclusive and semi-exclusive e^+e^- production in pp collisions at $\sqrt{s} = 7$ TeV*, JHEP **11** (2012) 080, arXiv:1209.1666 [hep-ex].
- [4] G. Aad *et al.*, (ATLAS Collaboration), *Measurement of exclusive $\gamma\gamma \rightarrow \ell^+\ell^-$ production in proton-proton collisions at $\sqrt{s} = 7$ TeV with the ATLAS detector*, Phys. Lett. **B749** (2015) 242, arXiv:1506.07098 [hep-ex].
- [5] A. M. Sirunyan *et al.*, (CMS and TOTEM Collaborations), *Observation of proton-tagged, central (semi)exclusive production of high-mass lepton pairs in pp collisions at 13 TeV with the CMS-TOTEM precision proton spectrometer*, CMS-PPS-17-001, TOTEM-2018-001, CERN-EP-2018-014, Submitted to: JHEP (2018) , arXiv:1803.04496 [hep-ex].
- [6] P. Lebiedowicz, R. Pasechnik, and A. Szczurek, *QCD diffractive mechanism of exclusive W^+W^- pair production at high energies*, Nucl. Phys. **B867** (2013) 61, arXiv:1203.1832 [hep-ph].
- [7] P. Lebiedowicz and A. Szczurek, *Exclusive production of heavy charged Higgs boson pairs in the $pp \rightarrow ppH^+H^-$ reaction at the LHC and a future circular collider*, Phys. Rev. **D91** (2015) 095008, arXiv:1502.03323 [hep-ph].
- [8] P. Lebiedowicz, M. Luszczak, R. Pasechnik, and A. Szczurek, *Can the diphoton enhancement at 750 GeV be due to a neutral technipion?*, Phys. Rev. **D94** no. 1, (2016) 015023, arXiv:1604.02037 [hep-ph].
- [9] M. Dyndal and L. Schoeffel, *The role of finite-size effects on the spectrum of equivalent photons in proton-proton collisions at the LHC*, Phys. Lett. **B741** (2015) 66, arXiv:1410.2983 [hep-ph].
- [10] W. Schäfer and A. Szczurek, *Exclusive photoproduction of J/ψ in proton-proton and proton-antiproton scattering*, Phys.Rev. **D76** (2007) 094014, arXiv:0705.2887 [hep-ph].
- [11] P. Lebiedowicz and A. Szczurek, *Exclusive $pp \rightarrow pp\pi^+\pi^-$ reaction: From the threshold to LHC*, Phys.Rev. **D81** (2010) 036003, arXiv:0912.0190 [hep-ph].
- [12] P. Lebiedowicz and A. Szczurek, *Revised model of absorption corrections for the $pp \rightarrow pp\pi^+\pi^-$ process*, Phys. Rev. **D92** (2015) 054001, arXiv:1504.07560 [hep-ph].
- [13] P. Lebiedowicz, O. Nachtmann, and A. Szczurek, *Central exclusive diffractive production of the $\pi^+\pi^-$ continuum, scalar, and tensor resonances in pp and p \bar{p} scattering within the tensor Pomeron approach*, Phys. Rev. **D93** (2016) 054015, arXiv:1601.04537 [hep-ph].
- [14] P. Lebiedowicz and A. Szczurek, *$pp \rightarrow ppK^+K^-$ reaction at high energies*, Phys.Rev. **D85** (2012) 014026, arXiv:1110.4787 [hep-ph].
- [15] P. Lebiedowicz, O. Nachtmann, and A. Szczurek, *Towards a complete study of central exclusive production of K^+K^- pairs in proton-proton collisions within the tensor Pomeron approach*, Phys. Rev. **D98** (2018) 014001, arXiv:1804.04706 [hep-ph].
- [16] P. Lebiedowicz, O. Nachtmann, and A. Szczurek, *Central exclusive diffractive production of p \bar{p} pairs in proton-proton collisions at high energies*, Phys. Rev. **D97** no. 9, (2018) 094027, arXiv:1801.03902 [hep-ph].

- [17] G. Baur, K. Hencken, and D. Trautmann, *Photon-photon physics in very peripheral collisions of relativistic heavy ions*, J. Phys. **G24** (1998) 1657, arXiv:hep-ph/9804348 [hep-ph].
- [18] V. Guzey and M. Zhalov, *Photoproduction of J/ψ and $\psi(2S)$ in proton-proton ultraperipheral collisions at the LHC*, arXiv:1405.7529 [hep-ph].
- [19] A. Cisek, W. Schäfer, and A. Szczurek, *Semiexclusive production of J/ψ mesons in proton-proton collisions with electromagnetic and diffractive dissociation of one of the protons*, Phys. Lett. **B769** (2017) 176, arXiv:1611.08210 [hep-ph].
- [20] G. G. da Silveira, L. Forthomme, K. Piotrkowski, W. Schäfer, and A. Szczurek, *Central $\mu^+\mu^-$ production via photon-photon fusion in proton-proton collisions with proton dissociation*, JHEP **02** (2015) 159, arXiv:1409.1541 [hep-ph].
- [21] M. Łuszczak, W. Schäfer, and A. Szczurek, *Two-photon dilepton production in proton-proton collisions: Two alternative approaches*, Phys. Rev. **D93** no. 7, (2016) 074018, arXiv:1510.00294 [hep-ph].
- [22] G. G. da Silveira and V. P. Goncalves, *Constraining the photon flux in two-photon processes at the LHC*, Phys. Rev. **D92** no. 1, (2015) 014013, arXiv:1506.01352 [hep-ph].
- [23] V. P. Goncalves, M. M. Jaime, D. E. Martins, and M. S. Rangel, *Exclusive and diffractive $\mu^+\mu^-$ production in pp collisions at the LHC*, Phys. Rev. **D97** no. 7, (2018) 074024, arXiv:1802.07339 [hep-ph].
- [24] I. G. Aznauryan *et al.*, (CLAS Collaboration), *Electroexcitation of nucleon resonances from CLAS data on single pion electroproduction*, Phys. Rev. **C80** (2009) 055203, arXiv:0909.2349 [nucl-ex].
- [25] V. I. Mokeev *et al.*, *New results from the studies of the $N(1440)1/2^+$, $N(1520)3/2^-$, and $\Delta(1620)1/2^-$ resonances in exclusive $ep \rightarrow e'p'\pi^+\pi^-$ electroproduction with the CLAS detector*, Phys. Rev. **C93** no. 2, (2016) 025206, arXiv:1509.05460 [nucl-ex].
- [26] L. Tiator and M. Vanderhaeghen, *Empirical transverse charge densities in the nucleon-to- $P_{11}(1440)$ transition*, Phys. Lett. **B672** (2009) 344, arXiv:0811.2285 [hep-ph].
- [27] G. Ramalho, *Analytic parametrizations of the $\gamma^*N \rightarrow N(1440)$ form factors inspired by light-front holography*, Phys. Rev. **D96** no. 5, (2017) 054021, arXiv:1706.05707 [hep-ph].
- [28] G. Ramalho and K. Tsushima, *$\gamma^*N \rightarrow N(1710)$ transition at high momentum transfer*, Phys. Rev. **D89** no. 7, (2014) 073010, arXiv:1402.3234 [hep-ph].
- [29] T. Gutsche, V. E. Lyubovitskij, and I. Schmidt, *Electromagnetic structure of nucleon and Roper in soft-wall AdS/QCD*, Phys. Rev. **D97** no. 5, (2018) 054011, arXiv:1712.08410 [hep-ph].
- [30] G. Ramalho and D. Melnikov, *Valence quark contributions for the $\gamma^*N \rightarrow N(1440)$ form factors from light-front holography*, Phys. Rev. **D97** no. 3, (2018) 034037, arXiv:1703.03819 [hep-ph].
- [31] H. F. Jones and M. D. Scadron, *Multipole $\gamma N - \Delta$ Form Factors and Resonant Photo- and Electroproduction*, Annals Phys. **81** (1973) 1.
- [32] T. A. Gail and T. R. Hemmert, *Signatures of chiral dynamics in the nucleon to Delta transition*, Eur. Phys. J. **A28** (2006) 91, arXiv:nucl-th/0512082 [nucl-th].
- [33] G. Ramalho, M. T. Pena, and F. Gross, *D-state effects in the electromagnetic $N\Delta$ transition*, Phys. Rev. **D78** (2008) 114017, arXiv:0810.4126 [hep-ph].
- [34] V. M. Budnev, I. F. Ginzburg, G. V. Meledin, and V. G. Serbo, *The two-photon particle production mechanism. Physical problems. Applications. Equivalent photon approximation*, Phys. Rept. **15** (1975) 181.
- [35] R. Fiore, A. Flachi, L. L. Jenkovszky, A. I. Lengyel, and V. K. Magas, *Explicit model realizing parton-hadron duality*, Eur. Phys. J. **A15** (2002) 505, arXiv:hep-ph/0206027 [hep-ph].
- [36] R. Fiore, A. Flachi, L. L. Jenkovszky, A. I. Lengyel, and V. K. Magas, *Kinematically complete analysis of the CLAS data on the proton structure function F_2 in a Regge-dual model*,

- Phys. Rev. **D69** (2004) 014004, arXiv:hep-ph/0308178 [hep-ph].
- [37] A. Szczurek and V. Uleshchenko, *Nonpartonic components in the nucleon structure functions at small Q^2 in the broad range of x* , Eur. Phys. J. **C12** (2000) 663, arXiv:hep-ph/9904288 [hep-ph].
 - [38] L. Forthomme, M. Łuszczak, W. Schäfer, and A. Szczurek, *Rapidity gap survival factors caused by remnant fragmentation for W^+W^- pair production via $\gamma^*\gamma^* \rightarrow W^+W^-$ subprocess with photon transverse momenta*, arXiv:1805.07124 [hep-ph].
 - [39] L. A. Harland-Lang, V. A. Khoze, and M. G. Ryskin, *Exclusive physics at the LHC with SuperChic 2*, Eur. Phys. J. **C76** no. 1, (2016) 9, arXiv:1508.02718 [hep-ph].
 - [40] I. Babiarz, R. Staszewski, and A. Szczurek, *Multi-parton interactions and rapidity gap survival probability in jet-gap-jet processes*, Phys. Lett. **B771** (2017) 532, arXiv:1704.00546 [hep-ph].
 - [41] V. A. Khoze, A. D. Martin, and M. G. Ryskin, *Multiple interactions and rapidity gap survival*, J. Phys. **G45** no. 5, (2018) 053002, arXiv:1710.11505 [hep-ph].
 - [42] L. Adamczyk. Private communication.